



**HAL**  
open science

## Speciation completion rates have limited impact on macroevolutionary diversification

Pierre Veron, Jérémy Andréoletti, Tatiana Giraud, Hélène Morlon

► **To cite this version:**

Pierre Veron, Jérémy Andréoletti, Tatiana Giraud, Hélène Morlon. Speciation completion rates have limited impact on macroevolutionary diversification. 2024. hal-04728750

**HAL Id: hal-04728750**

**<https://hal.science/hal-04728750v1>**

Preprint submitted on 9 Oct 2024

**HAL** is a multi-disciplinary open access archive for the deposit and dissemination of scientific research documents, whether they are published or not. The documents may come from teaching and research institutions in France or abroad, or from public or private research centers.

L'archive ouverte pluridisciplinaire **HAL**, est destinée au dépôt et à la diffusion de documents scientifiques de niveau recherche, publiés ou non, émanant des établissements d'enseignement et de recherche français ou étrangers, des laboratoires publics ou privés.



Distributed under a Creative Commons Attribution - NonCommercial 4.0 International License

1 A theoretical framework linking the birth-death  
2 and protracted birth-death models, with  
3 implications for the phylogenetic analysis of  
4 diversification

5 Pierre Veron <sup>1,2,\*</sup>, Jérémy Andréoletti <sup>1</sup>, Tatiana Giraud <sup>2</sup>, and  
6 Hélène Morlon <sup>1</sup>

7 <sup>1</sup>Institut de Biologie, École Normale Supérieure, Université PSL,  
8 CNRS, INSERM, Paris, France

9 <sup>2</sup>Écologie Systématique et Évolution, CNRS, Université Paris-Saclay,  
10 AgroParisTech, Gif-sur-Yvette, France

11 \*Corresponding author, [pveron@bio.ens.psl.eu](mailto:pveron@bio.ens.psl.eu)

12 July 1, 2024

13 **Keywords** speciation, macroevolution, microevolution, phylogeny

14 **Abstract**

15 While speciation takes time, standard birth-death processes used to infer diversifica-  
16 tion from phylogenies assume that it is instantaneous. This limits the interpretation  
17 of phylogenetic estimates of speciation and extinction rates, and our understanding of  
18 the microevolutionary processes that modulate these rates. Here, we consider the pro-  
19 tracted birth-death model, which accounts for the fact that speciation takes time. We  
20 compute an “equivalent” standard birth-death process, of which diversification dynam-  
21 ics approximate those induced by the protracted process. We find that the equivalent  
22 birth rate declines close to the present, and that the duration of speciation influences  
23 when this decays occurs more than the equivalent rates themselves. The equivalent  
24 rates are relatively constant in the past. The birth rate in the past scales with the rate  
25 at which speciation is initiated, with a scaling factor that depends mostly on the pop-  
26 ulation extinction rate. Our results suggest that the rates of speciation initiation and  
27 population extinction may often play a larger role than the speed at which populations  
28 acquire reproductive isolation in modulating speciation rates. Our study establishes a  
29 theoretical framework for understanding how microevolutionary processes combine to  
30 explain the diversification of species groups on macroevolutionary time scales.

## 31 **1 Introduction**

32 Birth-death models are widely used to understand the diversification of species groups;  
33 in this context, births represent speciation events, i.e. the emergence of two daughter  
34 species from a ancestral one, and deaths represent species extinction. This specific  
35 use of birth-death models is particularly widespread to interpret both fossil (Silvestro  
36 et al. 2014) and phylogenetic data (Stadler 2013; Morlon, Andréoletti, et al. 2024) in  
37 terms of diversification dynamics. In birth-death models, speciation is considered to be  
38 an instantaneous phenomenon, represented as a branching event following a Poisson  
39 point process.

40 Despite the widespread use of birth-death models to simulate speciation and extinction  
41 events, speciation is not instantaneous. Speciation requires an initial isolation of popu-  
42 lations (speciation initiation) followed by the accumulation of genetic barriers to gene  
43 flow until speciation is complete. Speciation can initiate and fail before completion,  
44 for example because of secondary contact, or because isolated populations go extinct  
45 before speciation completion (Coyne and Orr 2004; Dynesius and Jansson 2014). The  
46 whole speciation process may take hundreds of thousands up to several millions of  
47 years (Benton and Pearson 2001; Etienne and Rosindell 2012; Etienne, Morlon, et al.  
48 2014; Hua et al. 2022).

49 Ignoring the fact that speciation takes time by using standard birth-death models has  
50 non trivial consequences for our understanding of diversification dynamics. For exam-  
51 ple, when standard birth-death models are used in combination with phylogenetic trees  
52 of extant species to estimate speciation and extinction rates, the “protracted” nature of  
53 speciation may be misinterpreted as a speciation rate slowdown towards the present  
54 (Etienne and Rosindell 2012; Moen and Morlon 2014).

55 Etienne and Rosindell 2012 pioneered the development of the so-called protracted  
56 birth-death model (PBD). Instead of assuming that speciation is instantaneous as in the  
57 standard birth-death model, this model assumes that there are events of speciation *initi-*  
58 *ation* corresponding to the formation of *incipient* species that eventually become *good*  
59 species after a random *completion* time. An incipient lineage is a lineage that is not yet  
60 considered as a different species from the ancestral lineage. For sexually reproducing  
61 organisms, the completion time is the time it takes for lineages to achieve reproductive  
62 isolation. Each lineage is thus subject to initiation, extinction and completion events.

63 The protracted birth-death model has several advantages over the the standard birth-  
64 death model. First, it is biologically more realistic, and it thus unsurprisingly produces  
65 phylogenies that are closer to empirical phylogenies than those produced by the stan-  
66 dard birth-death model (Etienne and Rosindell 2012). Specifically, it produces phylo-  
67 genies that are less tippy (fewer recent speciation events) than those arising from the  
68 standard birth-death model. Second, it allows the integration of intraspecific processes  
69 that lead to speciation. For example, the matching competition birth-death model  
70 (MCBD, Aristide and Morlon 2019) integrates the effect of intraspecific competition  
71 on character displacement leading to speciation by modeling character displacement in  
72 incipient lineages.

73 Despite the advantages of the protracted birth-death model, the overwhelming major-  
74 ity of phylogenetic analyses of diversification use the standard birth-death model. Most  
75 available models for phylogenetic analyses of diversification are versions of the stan-  
76 dard birth-death model, with birth and death rates that can vary in time and/or across  
77 lineages (Morlon, Andréoletti, et al. 2024). The protracted birth-death model can be  
78 fitted to empirical phylogenies, however not all of its parameters can be reliably es-  
79 timated from a phylogeny (Etienne, Morlon, et al. 2014), which limits its usefulness.  
80 Recently, Hua et al. showed that the PBD parameters can be accurately estimated from  
81 population-level (rather than species-level) phylogenies, however such phylogenies re-  
82 main rare (Hua et al. 2022). Fitting standard birth-death models thus remains the rule  
83 in phylogenetic analyses of diversification.

84 If speciation takes time but it is estimated by fitting standard birth-death models to  
85 phylogenies, which assume instantaneous speciation, what do resulting speciation and  
86 extinction rate estimates actually represent? We can expect that speciation rate esti-  
87 mates will be higher when rates of speciation initiation and completion are higher, and  
88 rates of extinction of incipient species are lower, but precisely answering this question  
89 requires to establish an analytical relationship between the parameters of the protracted  
90 and standard birth-death models. To our knowledge, such a relationship has not yet  
91 been established.

92 Elucidating the relationship between the parameters of the protracted and standard  
93 birth-death models is important not only to clarify the meaning of speciation rates  
94 estimated from phylogenies, but also to understand the microevolutionary processes  
95 that modulate these rates (Morlon, Andréoletti, et al. 2024). Indeed, macroevolution-  
96 ary speciation rates (estimated from phylogenies) vary by orders of magnitude (Mali-  
97 et, Hartig, et al. 2019; Quintero et al. 2024), but the processes underlying this variation re-  
98 main unclear. Efforts to find empirical correlations between macroevolutionary specia-  
99 tion rates and rates of population formation or evolution of reproductive isolation have  
100 not been conclusive; a proposed explanation is that this expected correlation is erased  
101 by the frequent extinction of incipient species (Rabosky and Matute 2013; Singhal,  
102 Colli, et al. 2022; Singhal, Huang, et al. 2018). That is, population survival rather than  
103 population formation and the accumulation of reproductive barriers may be the factor  
104 “limiting” speciation. More generally, each of speciation initiation, speciation comple-  
105 tion and population survival may be the process limiting macroevolutionary speciation  
106 rates in some situations but not others (Rabosky 2016). For instance, a lineage that has  
107 a propensity to accumulate fast reproductive isolation but does not experience frequent  
108 population splits might not have a high speciation rate: here, the rate of speciation comple-  
109 tion is not limiting. Hence, factors acting on speciation initiation, the accumulation  
110 of reproductive isolation, and the extinction of incipient species can have non trivial  
111 outcomes in terms of speciation rate.

112 Here, we obtain a mathematical link between the parameters of the protracted and  
113 standard birth-death diversification models by computing “equivalent” speciation and  
114 extinction rates that generate some of the outcomes expected under the protracted birth-  
115 death model. In spirit, these equivalent rates are meant to represent the macroevolu-  
116 tionary outcomes (macroevolutionary speciation and extinction rates) of the protracted

117 birth-death process, as we may estimate them by fitting standard birth-death model to  
 118 reconstructed phylogenies. We compare phylogenies simulated under the protracted  
 119 birth-death model and the equivalent birth-death model and discuss the consequences  
 120 of our results for the phylogenetic analysis of diversification.

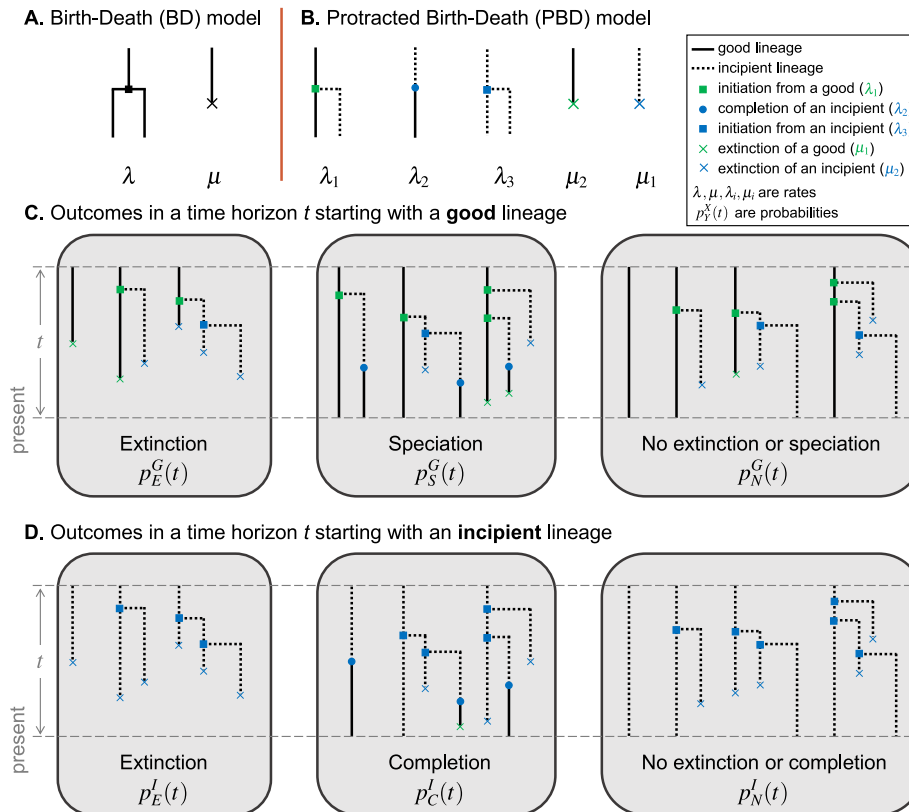


**Figure 1. The birth-death (BD) and protracted birth-death (PBD) models.** (A, B) Illustrations of the rates involved in the BD model (A), and the PBD model (B). (C, D) Possible outcomes of the PBD process in a fixed time horizon, starting from a good lineage (C) or an incipient lineage (D); non exhaustive examples of events leading to these outcomes are shown.

## 121 2 Materials and methods

### 122 2.1 Birth-death and protracted birth-death models

123 The standard birth-death (BD) model involves two rates (figure 1A): the birth (speciation)  
 124 rate  $\lambda$  and the death (extinction) rate  $\mu$ . The protracted birth-death (PBD) model  
 125 as defined in (Etienne, Mornon, et al. 2014) involves 5 rates (figure 1B) : the rate of  
 126 speciation initiation from a good species  $\lambda_1$ , the rate of completion  $\lambda_2$ , the rate of speciation  
 127 initiation from an incipient species  $\lambda_3$ , the rate of extinction of a good species

128  $\mu_1$ , and the rate of extinction of an incipient species  $\mu_2$ .

129 By convention, time elapses in the direction of increasing values. The process begins  
 130 at time 0 with one good lineage and runs until the present at time  $T$ . We now consider  
 131 an intermediate time  $T - t$ , and introduce  $p_E^G(t)$  and  $p_S^G(t)$  the probabilities that, for  
 132 any given good lineage, the first event is respectively an extinction or a speciation  
 133 event, and  $p_N^G(t)$  the probability that none of these events occur during a time interval  
 134 of length  $t$  (figure 1C). Similarly,  $p_E^I(t)$  and  $p_C^I(t)$  are the probabilities that, during a  
 135 time interval of length  $t$ , the first event is respectively an extinction, or a completion  
 136 event, when starting with an incipient lineage;  $p_N^I(t)$  is the probability that none of  
 137 these events occur during the time interval (figure 1D). By “extinction” we mean the  
 138 direct extinction of the lineage in question, or the extinction of all possible descendants  
 139 of this lineage in the time interval considered. Similarly, by “completion” we mean the  
 140 direct completion of the lineage in question, or the completion of an incipient daughter  
 141 lineage in the time interval under consideration. In case of multiple events occurring  
 142 in the time interval (e.g. speciation followed by extinction), we consider only the first  
 143 event. For instance the third case of speciation in figure 1C (where the lineages all go  
 144 extinct after speciation) is considered as a speciation event and is recorded in  $p_S^G(t)$ .

## 145 2.2 Equivalent time-dependent BD rates

### 146 Definitions of equivalent birth and death rates, and relation with probabilities of 147 speciation and extinction under the PBD

148 Given a PBD process with fixed parameter values running from 0 to  $T$ , we assume  
 149 that the probabilities of speciation and extinction within an infinitesimal time interval  
 150  $[t - dt, t]$  can be written as  $\hat{\lambda}(t) dt$  and  $\hat{\mu}(t) dt$ , for any time  $t$ . We call the quantities  $\hat{\lambda}(t)$   
 151 and  $\hat{\mu}(t)$  the time-dependent equivalent birth and death rates. Given a good lineage  
 152 alive at time  $T - t - dt$ , the probability that the first event occurring within the time  
 153 interval  $[T - t - dt, T]$  is a speciation event is given by:

$$154 \quad p_S^G(t + dt) = \underbrace{\hat{\lambda}(T - t) dt}_{(i)} + \underbrace{(1 - \hat{\lambda}(T - t) dt - \hat{\mu}(T - t) dt)}_{(ii)} \underbrace{p_S^G(t)}_{(iii)}$$

155 with (i) the probability of speciation within the small time interval  $[T - t - dt, T - t]$ ,  
 156 (ii) the probability of no speciation nor extinction within the small time interval  $[T - t -$   
 157  $dt, T - t]$  and (iii) the probability that the first event occurring within the time interval  
 158  $[T - t, T]$  is a speciation event, conditioned on existence of the lineage at the time  $T - t$ .  
 159 Similarly we have:

$$160 \quad p_E^G(t + dt) = \hat{\mu}(T - t) dt + (1 - \hat{\lambda}(T - t) dt - \hat{\mu}(T - t) dt) p_E^G(t).$$

161 Hence, we have the dynamical system

$$162 \quad \begin{cases} \frac{dp_S^G(t)}{dt} = \hat{\lambda}(T - t) - (\hat{\lambda}(T - t) + \hat{\mu}(T - t)) p_S^G(t) \\ \frac{dp_E^G(t)}{dt} = \hat{\mu}(T - t) - (\hat{\lambda}(T - t) + \hat{\mu}(T - t)) p_E^G(t) \end{cases}$$

163 which allows us to express the time-dependent birth rate:

$$164 \quad \hat{\lambda}(t) = \frac{(1 - p_E^G(T-t)) \left. \frac{dp_S^G}{dt} \right|_{T-t} + p_S^G(T-t) \left. \frac{dp_E^G}{dt} \right|_{T-t}}{p_N^G(T-t)} \quad (1)$$

165 and death rate:

$$166 \quad \hat{\mu}(t) = \frac{(1 - p_S^G(T-t)) \left. \frac{dp_E^G}{dt} \right|_{T-t} + p_E^G(T-t) \left. \frac{dp_S^G}{dt} \right|_{T-t}}{p_N^G(T-t)}. \quad (2)$$

167 In what follows, we compute the probabilities  $p_S^G(t)$  and  $p_E^G(t)$  for any time  $t \in [0, T]$ ,  
168 which provides us with the equivalent rates.

169 By assuming that the probabilities of speciation and extinction within an infinitesimal  
170 time interval  $[t - dt, t]$  can be written as  $\hat{\lambda}(t) dt$  and  $\hat{\mu}(t) dt$ , we have assumed that these  
171 probabilities depend only on time, and not on the history of the lineage considered.  
172 This is an approximation, because (under the PBD process) good lineages carry the  
173 history of their incipient species. An old lineage is indeed more likely to have a pool of  
174 incipient lineages (for instance, when  $\lambda_3$  is high, their number increases exponentially  
175 with time) and therefore less likely to go extinct. The equations we used for the prob-  
176 abilities of speciation  $p_S^G(t)$  and extinction  $p_E^G(t)$  correspond to the case of a good line-  
177 age with no incipient species, and are approximations otherwise. We expect that these  
178 approximations will affect mainly the extinction rate, as we ignore the buffering effect  
179 on extinction of incipient lineages that exist at the time when the rate is computed. The  
180 equivalent extinction rate could therefore overestimate extinction probabilities.

### 181 Speciation and extinction probabilities under the PBD

182 In order to compute  $p_S^G(t)$  and  $p_E^G(t)$  for any time  $t \in [0, T]$ , we first need to compute  
183 probabilities associated with incipient lineages.

184 Starting from an incipient lineage, the two exclusive possible ways leading to extinction  
185 within a horizon  $t$  are (figure 2, upper left panel): (a) the lineage directly goes extinct  
186 within a time  $t$  or (b) the lineage forms two incipient lineages after a time  $u \leq t$  and  
187 both incipient lineages go extinct within the remaining time  $t - u$ . The probability for  
188 an incipient lineage and its potential descendants to go extinct within a time  $t$  thus  
189 satisfies the following equation:

$$190 \quad p_E^I(t) = \frac{\mu_2}{\Lambda} (1 - e^{-\Lambda t}) \quad \text{figure 2(a)}$$

$$191 \quad + \int_0^t \lambda_3 e^{-\Lambda u} (p_E^I(t-u))^2 du \quad \text{figure 2(b)} \quad (3)$$

192 where  $\Lambda = \lambda_2 + \lambda_3 + \mu_2$ .

193 The solution to this integral equation is (appendix A1):

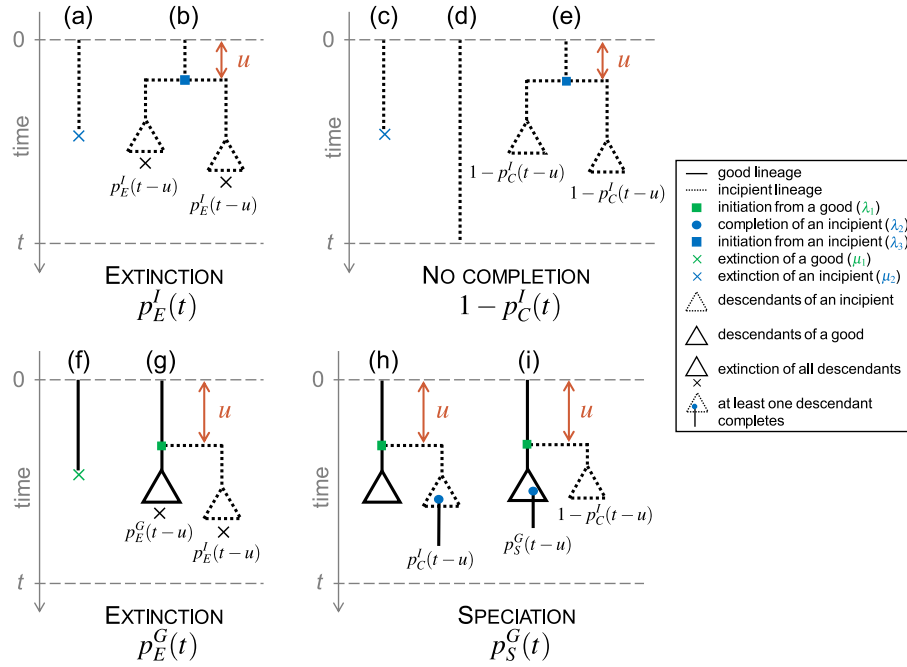


**Figure 2. Alternative scenarios by which main outcomes occur in the protracted birth-death model.** Upper panels: starting from an incipient lineage at time 0, decomposition of the possible exclusive ways of extinction (left) and no completion (right) before a given time  $t$ . Bottom panels: starting from a good lineage at time 0, decomposition of the possible exclusive ways of extinction (left) and speciation (right) before a given time  $t$ . Dotted lines represent incipient lineages, solid lines represent good lineages. Triangles summarize the subtrees containing the potential descendants of an ancestor lineage, with the condition that all of them go extinct within the remaining time (indicated by a cross), or that one of the completes speciation (indicated by a blue dot), or that none of these event occur. The probabilities written under the triangles correspond to the probability of the described event.

$$p_E^I(t) = \frac{1}{\lambda_3} \sqrt{\frac{c(\Lambda - k)e^{kt} + \Lambda/k}{(ce^{kt} + 1/k)^2} - \frac{\Lambda(k - \Lambda) + 2\mu_2\lambda_3}{2}}$$

$$\text{with } k = \sqrt{\Lambda^2 - 4\mu_2\lambda_3} \text{ and } c = \frac{2}{k - \Lambda} - \frac{1}{k}.$$

Instead of  $p_C^I(t)$ , it is easier to calculate  $1 - p_C^I(t)$ , the probability of non-completion. Starting from an incipient lineage, the three exclusive ways not to complete speciation are (figure 2, upper right panel): (c) direct extinction of the lineage within a time  $t$ , (d) survival of the lineage during a time  $t$  without completion, extinction or initiation, or (e) initiation of a good lineage after a time  $u \leq t$  and non-completion of any of the daughter lineages within the remaining time  $t - u$ . The probability of speciation completion of an incipient lineage (or any of its potential descendant) within a time  $t$  thus satisfies the following equation:



$$\begin{aligned}
 204 \quad 1 - p_C^I(t) &= \frac{\mu_2}{\Lambda} (1 - e^{-\Lambda t}) && \text{figure 2(c)} \\
 205 \quad &+ e^{-\Lambda t} && \text{figure 2(d)} \\
 206 \quad &+ \int_0^t \lambda_3 e^{-\Lambda u} (1 - p_C^I(t-u))^2 du && \text{figure 2(e)} \quad (4)
 \end{aligned}$$

207 This equation can be solved numerically by solving an ordinary differential equation  
 208 (appendix A2).

209 Starting now from a good lineage, the two exclusive possible ways leading to extinc-  
 210 tion as first event within a horizon  $t$  are (figure 2, bottom left panel): (f) the lineage  
 211 directly goes extinct within a time  $t$  or (g) the lineage forms an incipient lineage and  
 212 both daughter lineages (one good and one incipient) and their potential descendant  
 213 die within a time  $t - u$  without speciation. The probability for a good lineage and its  
 214 potential descendants to go extinct within a time  $t$  thus satisfies the following equation:

$$\begin{aligned}
 215 \quad p_E^G(t) &= \frac{\mu_1}{\Theta} (1 - e^{-\Theta t}) && \text{figure 2(f)} \\
 216 \quad &+ \int_0^t \lambda_1 e^{-\Theta u} p_E^I(t-u) p_E^G(t-u) du. && \text{figure 2(g)} \quad (5)
 \end{aligned}$$

217 where  $\Theta = \lambda_1 + \mu_1$ .

218 This equation can be solved numerically, provided that we already have a solution for  
 219  $p_E^I(t)$  (appendix A3).

220 Starting from a good lineage, the two exclusive ways in which speciation occurs within  
 221 a time  $t$  are (figure 2, bottom right panel): (h) the lineage initiates speciation after a  
 222 time  $u \leq t$ , and the incipient lineage completes speciation within the remaining time  
 223  $t - u$ , or (i) the lineage initiates speciation at a time  $u \leq t$ , the completion of this  
 224 incipient lineage fails, and the good lineage speciates within the remaining time  $t - u$ .  
 225 The probability that a good lineage fulfils speciation within a time  $t$  thus satisfies the  
 226 following equation:

$$\begin{aligned}
 227 \quad p_S^G(t) &= \int_0^t \lambda_1 e^{-\Theta u} \times && \text{initiation at time } u \\
 228 \quad &[p_C^I(t-u) && \text{figure 2(h)} \\
 229 \quad &+ (1 - p_C^I(t-u)) p_S^G(t-u)] du && \text{figure 2(i)} \quad (6)
 \end{aligned}$$

230 This equation can be solved numerically (appendix A4).

231 For all numerical integrations, we used the module `SciPy` in Python (Virtanen et al.  
 232 2020).

233 After solving these equations numerically and using equation 2, we obtain the time-  
 234 dependent equivalent birth rate  $\hat{\lambda}(t)$  and death rate  $\hat{\mu}(t)$ .

### 235 2.3 Equivalent constant BD rates

236 Defined, as above, as the values such that the probabilities of speciation and extinction  
237 in an infinitesimal time interval  $[t - dt, t]$  are given by  $\hat{\lambda}(t) dt$  and  $\hat{\mu}(t) dt$ , for any  
238 time  $t$  of the PBD process,  $\hat{\lambda}(t)$  and  $\hat{\mu}(t)$  indeed depend on time, even though the pa-  
239 rameters of the PBD are constant. However, as we will show later and in agreement  
240 with previous results (Etienne and Rosindell 2012), the time-dependency is particularly  
241 manifest towards the present. Intuitively, given enough time, constant rates of initia-  
242 tion, completion and extinction result in constant equivalent speciation and extinction  
243 rates. However, towards the present (i.e., towards the end of the PDB process), incip-  
244 ient lineages did not have enough time to complete speciation, resulting in a decline  
245 in speciation rates. As one of our main goals here is to understand how speciation  
246 initiation, completion and extinction translate into macroevolutionary speciation and  
247 extinction rates, we now introduce equivalent constant BD rates, meant to represent the  
248 relationship between the parameters of the PBD and BD process far from the present.

249 We define equivalent constant BD rates,  $\tilde{\lambda}$  (birth rate) and  $\tilde{\mu}$  (death rate) as the pa-  
250 rameters of the standard BD process such that the probability of speciation and the  
251 expected time to speciation match those under the PBD process with rates  $\lambda_1$ ,  $\lambda_2$ ,  $\lambda_3$ ,  
252  $\mu_1$ , and  $\mu_2$ , starting from a good lineage. The probability of extinction does not bring  
253 any additional information since extinction and speciation events are complementary  
254 over infinite time. Intuitively, we expect that the equivalent time-dependent birth and  
255 death rates tend towards  $\tilde{\lambda}$  and  $\tilde{\mu}$  in the past; the equivalent time-dependent birth rate  
256 then declines toward the present.

257 We shown that equivalent constant-time rates are given by the following expressions  
258 (see details [appendix A5](#)):

$$259 \quad \tilde{\lambda} = (1 - \pi)\lambda_1 \quad \text{and} \quad \tilde{\mu} = \mu_1 \quad (7)$$

260 where  $\pi = \frac{\lambda_2 + \lambda_3 + \mu_2}{2\lambda_3} \left(1 - \sqrt{1 - 4 \frac{\lambda_3 \mu_2}{(\lambda_2 + \lambda_3 + \mu_2)^2}}\right)$  is the probability of non-completion of  
261 an incipient lineage.

262 [Equation 7](#) shows that, far from the present, the equivalent death rate is exactly the rate  
263 of extinction of good species, and the equivalent birth rate is directly proportional to the  
264 rate of speciation initiation from a good species, with a coefficient of proportionality  
265 that represents the probability of completion without time horizon and depends on the  
266 rates specific to incipient lineages (initiation, completion and extinction). As in the case  
267 of the time-dependent equivalent rates, these rates correspond to the case of a process  
268 starting with a good lineage without incipient lineages, and the equivalent extinction  
269 rate may thus overestimate actual extinction probabilities under the PBD.

270 In order to better understand the influence of each parameter of the PBD process on the  
271 equivalent constant birth rate  $\tilde{\lambda}$ , we calculate partial derivatives of this function with  
272 respect to the different parameters. A high partial derivative with respect to a given  
273 parameter reflects a strong influence of this parameter on the equivalent birth rate, and  
274 therefore that the corresponding step of the speciation process may be limiting. We  
275 compute the relative influence of a given parameter as the ratio between the absolute

276 partial derivative with respect to this parameter and the sum of the absolute partial  
277 derivatives with respect to all other parameters. We perform these analyses both for  
278 the simplified PBD model where good and incipient lineages have the same rates of  
279 initiation ( $\lambda_1 = \lambda_3$ ) and extinction ( $\mu_1 = \mu_2$ ) and for the full PBD model. Detailed  
280 calculations are provided in [appendix A6](#).

## 281 **2.4 Simulations under the PBD process and equivalent BD pro-** 282 **cesses**

283 Although the equivalent rates were designed to construct BD processes that approach  
284 the PBD process, these processes are not identical. We used simulations to compare  
285 reconstructed trees (i.e., trees of extant species) generated by the PBD process and their  
286 equivalent BD processes. In each of these simulations, we consider the trees of extant  
287 good species, disregarding extinct and incipient lineages. We compared trees simulated  
288 under the constant-rate PBD model with trees simulated under the corresponding time  
289 constant (BD) and time-varying BD model (varBD). We independently varied each of  
290 the 5 parameters of the PBD model, each taking 5 values (the default value and 2 above,  
291 2 below, with amplitude chosen to guarantee computational tractability), resulting in  
292 25 parameter combinations. For each combination, we computed the trajectories of  
293 equivalent time-dependent birth and death rates over 15 million years – approximated  
294 by piecewise-constant birth and death rates over 200 intervals – and simulated 500  
295 tree replicates using the R library [TreeSim](#) (Stadler 2011). The values of these rates  
296 are given in supplementary figure S4. Each tree simulation was conditioned on the  
297 survival of two extant lineages (up to the failure of 100 simulation attempts for each  
298 replicate), starting from a single stem branch. We also generated the same number of  
299 trees under the PBD model for each combination of parameters using the [PBD](#) package  
300 (Etienne and Rosindell 2012). Finally, we simulated trees under the BD model with  
301 equivalent constant rates, using the package [TreeSim](#). We expect these simulations to  
302 deviate the most from those obtained under the PBD process. We compared the outputs  
303 of the simulations under the three models in terms of species richness at present (SR),  
304 tree shape and tree topology.

305 To analyze tree shape, we used the  $\gamma$  statistic (Pybus and Harvey 2000), computed with  
306 the package [ape](#) (Paradis and Schliep 2019). The  $\gamma$  statistic quantifies the relative  
307 position of the internal nodes of a tree and compares it to the expectations under a  
308 pure-birth (Yule) model.  $\gamma > 0$  corresponds to trees where internal nodes are closer  
309 to the tips than expected under Yule’s model, while  $\gamma < 0$  corresponds to trees where  
310 internal nodes are closer to the root.

311 To analyze tree topology, we used the stairs2 balance index (Norström et al. 2012),  
312 computed with the package [treestats](#) (Janzen and Etienne 2024). This statistic mea-  
313 sures the mean size ratio between the smaller and larger pending subtree for all vertices.  
314 Stairs2 is higher for trees with more balanced subtrees and lower for more imbalanced  
315 trees. The stairs2 statistic has been shown to perform well (Khurana et al. 2023) and is  
316 less sensitive to tree size than other statistics such as Aldous’  $\beta$  (Aldous 2001).

## 317 **2.5 Ability to recover equivalent constant BD rates by fitting the** 318 **BD model to truncated trees**

319 If we acknowledge that speciation in nature usually takes time, birth and death rates  
320 estimates obtained by fitting a constant-rate BD model to empirical reconstructed trees  
321 are hard to interpret. As noted above, under a constant rate PBD model, we expect  
322 equivalent birth rates to approach the equivalent constant birth rate  $\tilde{\lambda}$  in the past, and  
323 to decline closer to the present. Hence, we can expect that speciation rate estimates  
324 obtained by fitting a BD model to the entire tree will have intermediate values below  
325  $\tilde{\lambda}$ . However, fitting a BD model to older parts of the tree should provide good  
326 estimates of the equivalent constant BD rates.

327 To test this expectation, we truncated the phylogenies simulated under the PBD process  
328 in [section 2.4](#) at different time points in the past, and fitted a constant BD model to these  
329 truncated phylogenies, using the dedicated function `fit_bd_in_past` (Lewitus et al.  
330 [2018](#); Perez-Lamarque et al. [2022](#)) from the R package `RPANDA` (Morlon, Lewitus, et  
331 al. [2016](#)). We fitted a constant-rate birth-death model to both entire trees and truncated  
332 trees “sliced” at 17 regularly spaced time points between the present and 4 million years  
333 before the present. Finally, we compared the speciation and extinction rates estimates  
334 obtained with various truncation times to the analytically-derived equivalent constant  
335 BD rates.

## 336 **3 Results**

### 337 **3.1 Equivalent time-dependent BD rates**

338 We used [equations 1](#) and [2](#) and numerical solutions of the equations describing the  
339 probabilities of speciation, completion and extinction with time to derive equivalent  
340 time-dependent birth and death rates (thereafter simply referred to as birth and death  
341 rates) for a large range of parameter values.

342 We find that birth rates decrease close to the present, reaching 0 at present (time  $t \rightarrow T$ ,  
343 see [figure 3](#)). Death rates depend less on time and can be considered almost constant  
344 with time if we neglect a small decrease followed by a short increase when  $t \rightarrow T$ . In  
345 the past ( $t \rightarrow 0$ ), birth and death rates converge to the values predicted by our analytical  
346 expression of the equivalent constant BD rates ([equation 7](#)). This provides indirect  
347 (graphical) evidence that the constant equivalent birth-death rates can be considered as  
348 asymptotic rates of the time-dependent equivalent birth-death rates.

349 Initiation rates have a strong effect on the birth rate ([figure 3](#), panel **A**). In the past, birth  
350 rates converge to values scaling with the initiation rate, all other rates being equal, as  
351 expected from [equation 7](#). As expected, lower completion rates result in lower birth  
352 rates, and an effect of the protracted nature of speciation that extends further into the  
353 past (panel **C**). In the limit  $\lambda_2 \rightarrow \infty$ , the model converges to a pure BD model with  
354 constant rates, except very close to the present. Indeed, with high completion rates,  
355 incipient lineages complete speciation very fast and with high probability, so specia-  
356 tion occurs as soon as an initiation event occurs. Finally, birth rates are lower when

357 extinction rates are higher, except closer to the present where the effect of extinction  
358 diminishes (panel **E**). This effect is entirely due to the extinction of incipient lineages  
359 ( $\mu_2$ ), as the extinction rate of good lineages ( $\mu_1$ ) has virtually no effect on the birth  
360 rate (supplementary figure S2). The higher extinction rate of incipient lineages ren-  
361 ders speciation less likely, as incipient species more often go extinct before completing  
362 speciation.

363 Death rates match closely extinction rates (figure 3, panel **F**), entirely due to the effect  
364 of the extinction rate of good lineages, as expected from equation 7; indeed, the ex-  
365 tinction rate of incipient lineages has no effect on the death rate (supplementary figure  
366 S2).

### 367 **3.2 Equivalent constant BD rates**

368 As shown by equation 7 and already described above, the equivalent constant death  
369 rate equals the extinction rate of good species; the equivalent constant birth rate scales  
370 with speciation initiation, it increases with the completion rate and decreases with the  
371 extinction rate of incipient lineages (figure 3, dashed lines). We better characterized  
372 the influence of each step of the speciation process (i.e., initiation, survival of incipient  
373 species, and completion) on  $\tilde{\lambda}$ , interpreted as the macroevolutionary speciation rate,  
374 by computing relative partial derivatives. This allows us to identify the steps of the  
375 PBD process that may limit macroevolutionary speciation rates figure 4. We identify  
376 that speciation initiation is limiting when its rate is low and the completion rate is high  
377 (regions 1 and 2). Speciation completion is limiting when its rate is low compared to  
378 the other parameters (regions 3 and 5). An increase in the population extinction rate has  
379 most effects when this rate is low (region 6) and when initiation rate is high compared  
380 to the completion rate (regions 4 and 5).

### 381 **3.3 Trees generated by the PBD process and equivalent BD pro-** 382 **cesses**

383 We compared the size, shape and topology of trees generated under the PBD model  
384 to those of trees generated under their equivalent time-constant and time-varying BD  
385 models (figure 5). As expected, tree size (SR) increases with higher rates of specia-  
386 tion initiation and completion, and decreases with higher rates of extinction of good  
387 and incipient lineages (figure 5, top row). These trends are well captured by both the  
388 equivalent time-varying and time-constant models, with the exception of the increase  
389 in species richness with the rate of initiation from incipient lineages  $\lambda_3$ . Compared to  
390 the PBD model, the equivalent BD models produce larger trees when  $\lambda_3$  is small, and  
391 smaller trees when  $\lambda_3$  is large.  $\lambda_3$  has little influence on the size of trees generated un-  
392 der equivalent BD models, consistently with the weak influence of  $\lambda_3$  on the equivalent  
393 rates (see supplementary figure S3C and **D**).

394 As expected given unachieved speciation close to the present, the PBD process results  
395 in trees with negative  $\gamma$  values (reflecting long terminal branches), unless the comple-  
396 tion or extinction rates are high (figure 5, middle row).  $\gamma$  decreases with increasing  
397 ratios of speciation initiation to speciation completion rates, i.e. when the protracted

398 nature of the speciation process is more pronounced). The equivalent variable-rate BD  
399 model captures these trends relatively well, while the constant-rate BD model produces  
400 trees with positive  $\gamma$  values, indicating nodes closer to the tips. The drop towards 0 in  
401 the equivalent time-variable birth rates captures the shortage of speciation events close  
402 to the present induced by the protracted process, except when the rate of initiation from  
403 an incipient lineage ( $\lambda_3$ ) gets large. In this case the PBD process produces trees with  
404 increasingly long branch lengths, while the distribution of nodes generated under the  
405 equivalent time-dependent BD model remains stable.

406 Under most PBD parameters, stairs2 values of tree topology are stable, close to 0.65,  
407 and well reproduced by both the time-constant and the time-variable equivalent BD  
408 models. Higher values of stairs2 (reflecting more balanced trees) are observed in pa-  
409 rameter ranges leading to small trees, and likely reflect tree size rather than a true  
410 difference in tree balance.

411 Deviations observed between trees simulated under the PBD process and those simu-  
412 lated under the equivalent time-varying BD model under some  $\lambda_3$  values likely come  
413 from the approximation we made when establishing the link between equivalent rates  
414 and the probabilities of speciation and extinction under the PBD (see [section 2.2](#)). If,  
415 as expected, the equivalent extinction rate overestimate extinction probabilities, this  
416 explains why we obtain smaller trees with less negative gamma values, as extinction  
417 pushes nodes towards the present (the “pull of the present”, Nee et al. 1994). This is  
418 especially pronounced if  $\lambda_3$  is high when the approximation is the strongest, as there  
419 are many incipient lineages that are not accounted for (the ones that originated before  
420 the time at which the rates are calculated).

### 421 **3.4 Recovery of equivalent BD rates by fit to truncated PBD trees**

422 Our expectation that fits of a constant rate BD model to the “old” part of trees generated  
423 under a PBD process would provide good estimates of the equivalent BD rates was  
424 verified (supplementary figures S7a and S7b). When fitting a constant rate BD model  
425 to the entire tree (i.e., when the truncation time is zero), the estimated speciation and  
426 extinction rates are well below the expected equivalent constant rates. However when  
427 truncation time increases, these estimates converge to the expected equivalent rates. In  
428 the case of the extinction rate, estimates remain slightly below the expected equivalent  
429 rate, supporting our intuition that equivalent extinction rates should overestimate actual  
430 extinction events. The convergence occurs with a truncation time relatively close to the  
431 present, consistent with the observed time of decline of the equivalent time-dependent  
432 BD rates. This recent truncation time appears optimal, as estimates are not as good  
433 when more of the tree is truncated, probably due to a loss of statistical power with  
434 decreasing data size.

## 435 **4 Discussion**

436 In this study we derived predictions, under the protracted birth-death (PBD) model of  
437 diversification, for “equivalent” birth and death rates, meant to represent macroevolu-

438 tionary speciation and extinction rates as we may estimate them from reconstructed  
439 phylogenies. The protracted birth-death model accounts for the fact that speciation is  
440 not an instantaneous process and decorrelates the process of speciation initiation and  
441 speciation completion. The first process can be understood by a rate at which a lineage  
442 creates incipient lineages and the second process is characterized by a completion rate,  
443 i.e. a rate at which these lineages will become distinct species (denoted as *good* species  
444 in the model). We showed that the equivalent rates – in particular the birth rate – vary  
445 when the process approaches the present, but can be considered constant when far from  
446 the present. Our analytical predictions of the rates in the past allowed us to explore the  
447 importance of each step of the speciation process (i.e. initiation, survival, comple-  
448 tion) in modulating the macroevolutionary speciation rate. In addition, we showed that  
449 macroevolutionary speciation rates estimated on truncated reconstructed trees can pro-  
450 vide good estimates of the equivalent birth rate. This opens the possibility to relate es-  
451 timates of macroevolutionary speciation rates, which have major consequences for the  
452 build up of diversity over geological time scales, to the microevolutionary processes  
453 that modulate speciation initiation, population survival, and speciation completion.

454 As expected given previous results on the protracted birth-death process (Etienne and  
455 Rosindell 2012), we find that equivalent birth rates decline to zero as time approaches  
456 the present. Close to the present, speciation is less likely to occur because it requires  
457 a delay. The decay in equivalent birth rate starts earlier when the completion rate is  
458 lower. Trees simulated under the equivalent time-dependent BD model have similar  
459 characteristics to trees simulated under the PBD process, in terms of tree size and  
460 shape (figure 5), meaning that the equivalent BD process captures the dynamics of  
461 speciation and extinction induced by the protracted model relatively well. It is however  
462 important to remember that the PBD and equivalent BD processes are not entirely  
463 interchangeable. The PBD process is a process with memory, which induces an age  
464 dependency of speciation and extinction rates that is not captured by the equivalent  
465 BD process. For example “old” species are more likely to have accumulated incipient  
466 lineages, which buffer their extinction risk, but this cannot be captured by an age-  
467 independent BD process. More generally, the approximations made in our equivalent  
468 BD process lead to an overestimation of extinction events occurring under the PBD  
469 process, explaining some of the deviations observed when comparing simulated trees,  
470 in particular for high values of the rate of initiation from incipient lineages ( $\lambda_3$ ).

471 Before equivalent speciation rates start to drop, they can be considered virtually con-  
472 stant. In this regime, we derived analytical relationships between the equivalent birth  
473 and death rates and the parameters of the PBD process. These relationships show that  
474 we can expect macroevolutionary extinction rates to provide a relatively good approx-  
475 imation of the rate at which species go extinct, except if the rate of initiation from  
476 incipient lineages is large. They also show that macroevolutionary speciation rates are  
477 directly proportional to speciation initiation rates, with a coefficient of proportionality  
478 that depends on the rates of completion, initiation and extinction of incipient lineages.  
479 Hence, all aspects of the speciation process play a role in modulating macroevolution-  
480 ary speciation rates, but some play a larger role than others, and which ones will likely  
481 depend on the ecology, genetics and biogeography of the species group considered.  
482 Indeed, by identifying regimes within which each aspect of the speciation process is

483 expected to be the most influential (figure 4), we found that the rates of speciation ini-  
484 tiation and population extinction often are the limiting factors. Completion rates are  
485 only limiting when they are very small and at intermediate values of speciation initia-  
486 tion rates, or high population extinction rates. Hence, a species that accumulates fast  
487 reproductive isolation will be characterized by a higher completion rate but this will  
488 not necessarily have a strong effect on the speciation rate (figure 3C).

489 Our results have implications for the phylogenetic analysis of diversification. Indeed,  
490 ignoring the fact that speciation takes time by fitting standard BD models to empirical  
491 phylogenies necessarily leads to model misspecification (e.g. when fitting a constant  
492 rate BD model) or misinterpretation (e.g. when interpreting the effect of protraction as  
493 a speciation rate decline). In the recent years, there has been a surge in the use of tip-  
494 rate speciation estimates, i.e. estimates of speciation rates at present across the tips of a  
495 phylogeny, obtained with statistics such as the diversification rate (DR; Jetz et al. 2012)  
496 statistic, or models such as Bayesian analysis of macroevolutionary mixtures (BAMM;  
497 Rabosky 2014), the cladogenetic diversification shift (ClaDS; Maliet, Hartig, et al.  
498 2019; Maliet and Morlon 2021), or birth-death diffusion (BDD; Quintero et al. 2024)  
499 models. Future work investigating how speciation rates estimated with these methods  
500 on trees generated under the PBD process compare with equivalent rates will be useful.  
501 However the fact that equivalent birth rates converge to zero close to the present sug-  
502 gests that tip rate estimates provide a poor representation of speciation probabilities.  
503 Speciation rates estimated on deeper parts of the phylogeny approximate equivalent  
504 rates quite well, suggesting that these estimates indeed reflect the macroevolutionary  
505 outcome of the combined processes of initiation, survival and completion. Ideally, we  
506 would need to account for the protracted nature of speciation in every model used to  
507 infer diversification rates from phylogenies. While progress is being made in this di-  
508 rection (Hua et al. 2022), it adds substantial computational complexity. A workaround  
509 is to truncate phylogenies; however this requires employing inference methods that  
510 account for this truncation. These have been implemented for only a limited set of  
511 models, such as the constant-rate, time-dependent and environment-dependent models  
512 developed in RPANDA (Morlon, Lewitus, et al. 2016). More systematically implement-  
513 ing this truncation option in diversification models would be useful. Our tests indicate  
514 that truncating phylogenetic trees at intermediate time points yields the most accurate  
515 estimates of equivalent rates. As the optimal truncation time will depend on the extent  
516 to which speciation is protracted (i.e., the completion rate), we recommend to apply  
517 truncation at various time points and chose the time at which the estimated rates reach  
518 a plateau.

519 Our results also have implications for the ongoing effort to relate macroevolutionary  
520 speciation rates to microevolutionary processes (Rolland et al. 2023; Harvey et al.  
521 2019; Rabosky 2016). Indeed, microevolutionary processes act individually on each  
522 step of the speciation process (initiation, survival, completion), and our expressions of  
523 equivalent rates provide an idea of how these combine to modulate macroevolutionary  
524 speciation rates. For example, the apparent absence of correlation between tip rate esti-  
525 mates of speciation and the speed at which reproductive isolation is acquired (Rabosky  
526 and Matute 2013; Freeman et al. 2022) is not surprising given our expectation that  
527 completion rates have a limited effect on the macroevolutionary speciation rate (and



528 the limitations of tip rate estimates mentioned before). We however expect to find a  
529 correlation between macroevolutionary speciation rates and the rate of population for-  
530 mation, which reflects speciation initiation. This is indeed what was found by Harvey  
531 et al. 2019; the lack of correlation in other studies (Singhal, Colli, et al. 2022; Singhal,  
532 Huang, et al. 2018; Burbink et al. 2023) may reflect cases when speciation is modu-  
533 lated by the rate of population extinction rather than by the rate of speciation initiation,  
534 as expected if the initiation rate is high and/or the population extinction rate is low.

535 By accounting for the time it takes to complete speciation, protracted birth-death mod-  
536 els provide more biologically realistic models than standard birth-death models, and a  
537 theoretical framework for understanding how each step of the speciation processe influ-  
538 ences macroevolutionary speciation rates. A more systematic account of the protracted  
539 nature of speciation in phylogenetic analyses of diversification would both improve  
540 our estimates of diversification rates and our understanding of how microevolutionary  
541 processes combine to modulate macroevolutionary speciation rates.

## 542 **Code availability**

543 The scripts used to make these analyses are available on [https://github.com/](https://github.com/pierre-veron/PBD_analog)  
544 [pierre-veron/PBD\\_analog](https://github.com/pierre-veron/PBD_analog).

## 545 **Acknowledgement**

546 We thank Thibault Juillard, Amandine Véber and Amaury Lambert for mathematical  
547 advice; and Benoît Perez-Lamarque who kindly shared his code to estimate the BD  
548 rates on truncated phylogenies.

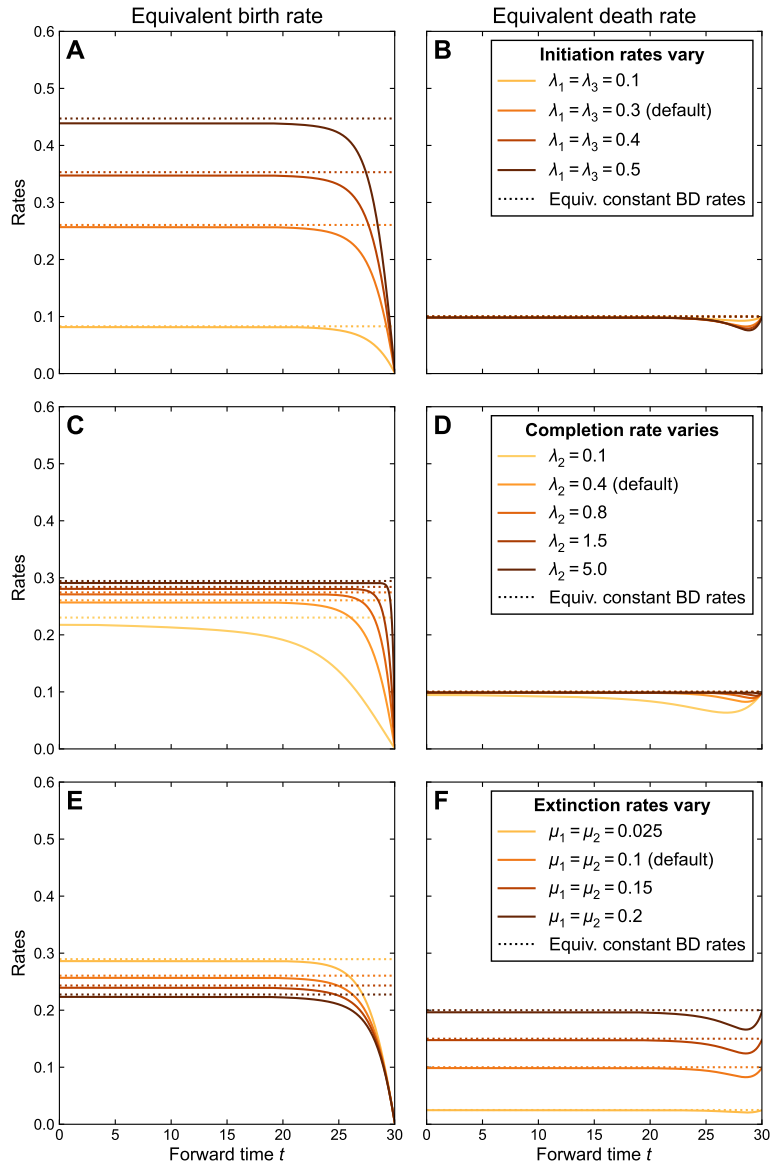


**Figure 3. Influence of the parameters of the protracted birth-death (PBD) process on equivalent birth-death (BD) rates.** Solid lines represent equivalent BD rates derived from equations 1 and 2 as a function of time for different values of PBD rates. Dotted lines represent constant equivalent BD rates derived analytically from equation 7 for the same PBD parameters. In the top/middle/bottom row the initiation/completion/extinction rates vary, with the other rates constant (default values are  $\lambda_1 = \lambda_3 = 0.3, \lambda_2 = 0.4, \mu_1 = \mu_2 = 0.1$ ). In figures S2 and S3, we calculated the same rates with the 5 parameters varying independently.  $t = 30$  corresponds to the present,  $t = 0$  to the past.

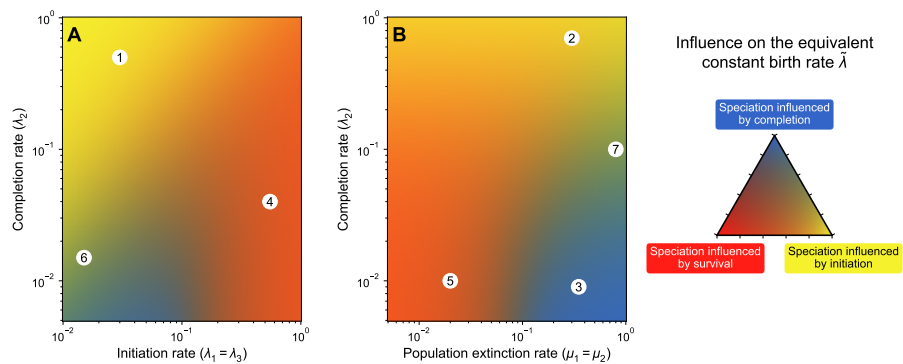


**Figure 4. Relative influence of the parameters of the PBD model on the equivalent constant birth rate.** Colors indicate which of the PBD process among initiation, completion and population extinction limits the equivalent constant birth rate  $\bar{\lambda}$  most, as a function of (A) the initiation and completion rates and (B) the population extinction and completion rates, with the color code explained on the triangle in the right. A yellow region (e.g. 1 or 2) indicates a combination of parameters where the most influential parameter on the birth rate is the rate of initiation. A blue region (e.g. 3) indicates a combination of parameters where the most influential parameter is the rate of completion  $\lambda_2$ . A orange region (e.g. 4 or 5) indicates a combination of parameters where both population extinction and speciation initiation are influential. Green regions (e.g. 6 or 7) indicate situations where both speciation initiation and completion have a similar influence on the birth rate. In all cases, the rates of initiation and completion have a positive influence on the birth rate and the rate of population extinction has a negative influence. The detailed methods are explained in [appendix A6](#) and the values of the relative influence are provided in supplementary figure S5. When they do not vary, default values of the parameters are 0.1.

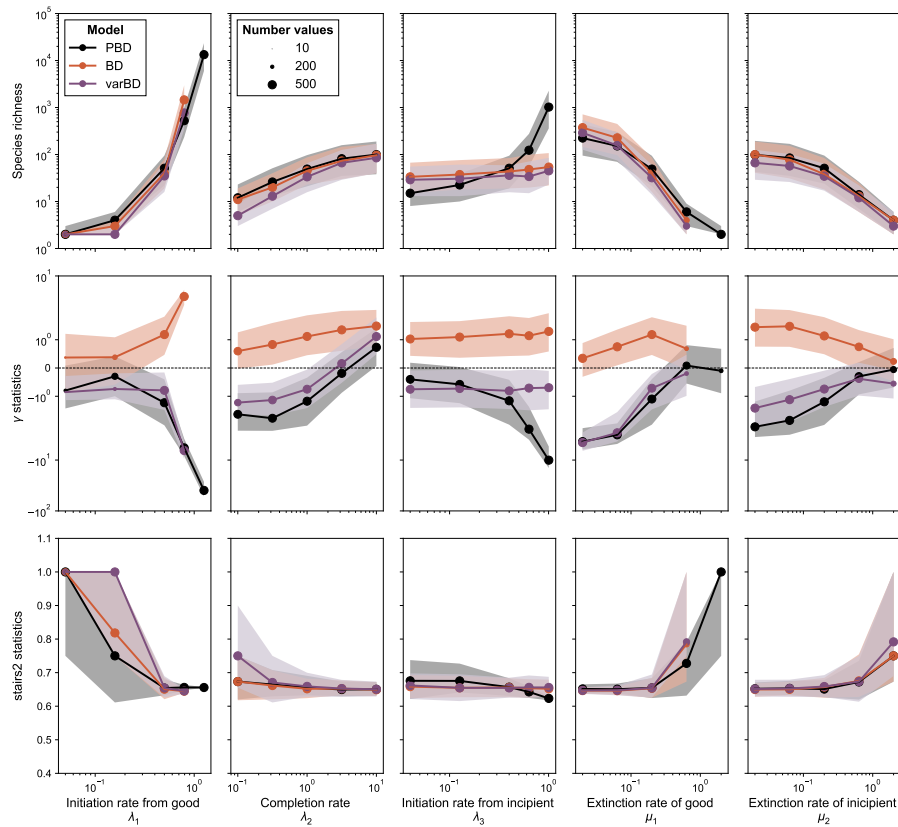


**Figure 5. Statistics of trees generated under the protracted birth-death (PBD) process and its equivalent birth-death (BD) processes.** By row: species richness SR,  $\gamma$  shape statistic and stairs2 balance index for trees generated under the three models (PBD, equivalent constant rate BD and equivalent time varying rate BD) for different values of the parameters of the PBD model. In each column, only one of the PBD parameters varies, with the others held constant (default  $\lambda_1 = 0.5$ ,  $\lambda_2 = 1.0$ ,  $\lambda_3 = 0.4$ ,  $\mu_1 = 0.2$ ,  $\mu_2 = 0.2$ ). For each set of parameters of the PBD model, BD and varBD trees were generated under equivalent birth and death rates computed using equations 1, 2 and 7. The line corresponds to the median of statistics across all 200 replicates, the shaded area indicates the first and last quartile of the statistics. The size of the dots indicates the number of valid data for which the statistics could be calculated.

## 549 References

- 550 Aldous, David J. (2001). “Stochastic models and descriptive statistics for phylogenetic  
551 trees, from Yule to today”. In: *Statistical Science* 16.1, pp. 23–34. DOI: [10.1214/  
552 ss/998929474](https://doi.org/10.1214/ss/998929474).
- 553 Aristide, Leandro and H el ene Morlon (2019). “Understanding the effect of competition  
554 during evolutionary radiations: an integrated model of phenotypic and species diver-  
555 sification”. In: *Ecology Letters* 22.12, pp. 2006–2017. DOI: [10.1111/ele.13385](https://doi.org/10.1111/ele.13385).
- 556 Benton, Michael J. and Paul N. Pearson (2001). “Speciation in the fossil record”.  
557 In: *Trends in Ecology and Evolution* 16.7, pp. 405–411. DOI: [10.1016/s0169-  
558 5347\(01\)02149-8](https://doi.org/10.1016/s0169-5347(01)02149-8).
- 559 Burbrink, Frank T., Sara Ruane, Nirhy Rabibisoa, Achille P. Raselimanana, Christo-  
560 pher J. Raxworthy, and Arianna Kuhn (2023). “Speciation rates are unrelated to the  
561 formation of population structure in Malagasy gemsnakes”. In: *Ecology and Evolu-  
562 tion* 13.8, e10344. DOI: [10.1002/ece3.10344](https://doi.org/10.1002/ece3.10344).
- 563 Coyne, Jerry A. and H. Allen Orr (2004). *Speciation*. Sunderland, Massachusetts: Sin-  
564 auer Associates, Inc. Publ. 545 pp. ISBN: 0878930892.
- 565 Dynesius, Mats and Roland Jansson (2014). “Persistence of within-species lineages:  
566 A neglected control of speciation rates”. In: *Evolution* 68.4, pp. 923–934. DOI: [10.  
567 1111/evo.12316](https://doi.org/10.1111/evo.12316).
- 568 Etienne, Rampal S., H el ene Morlon, and Amaury Lambert (2014). “Estimating the  
569 duration of speciation from phylogenies”. In: *Evolution* 68.8, pp. 2430–2440. DOI:  
570 [10.1111/evo.12433](https://doi.org/10.1111/evo.12433).
- 571 Etienne, Rampal S. and James Rosindell (2012). “Prolonging the Past Counteracts the  
572 Pull of the Present: Protracted Speciation Can Explain Observed Slowdowns in Di-  
573 versification”. In: *Systematic Biology* 61.2, pp. 204–213. DOI: [10.1093/sysbio/  
574 syr091](https://doi.org/10.1093/sysbio/syr091).
- 575 Freeman, Benjamin G., Jonathan Rolland, Graham A. Montgomery, and Dolph Schlut-  
576 ter (2022). “Faster evolution of a pre-mating reproductive barrier is not associated  
577 with faster speciation rates in New World passerine birds”. In: *Proceedings of the  
578 Royal Society B* 289.1966, p. 20211514. DOI: [10.1098/rspb.2021.1514](https://doi.org/10.1098/rspb.2021.1514).
- 579 Harvey, Michael G., Sonal Singhal, and Daniel L. Rabosky (2019). “Beyond Reproduc-  
580 tive Isolation: Demographic Controls on the Speciation Process”. In: *Annual Review  
581 of Ecology, Evolution, and Systematics* 50.1, pp. 75–95. DOI: [10.1146/annurev-  
582 ecolsys-110218-024701](https://doi.org/10.1146/annurev-ecolsys-110218-024701).
- 583 Hua, Xia, Tyara Herdha, and Conrad J. Burden (2022). “Protracted Speciation under  
584 the State-Dependent Speciation and Extinction Approach”. In: *Systematic Biology*  
585 71 (6), pp. 1362–1377. DOI: [10.1093/sysbio/syac041](https://doi.org/10.1093/sysbio/syac041).
- 586 Janzen, Thijs and Rampal S. Etienne (2024). “Phylogenetic tree statistics: a systematic  
587 overview using the new R package ‘treestats’”. In: *bioRxiv*. DOI: [10.1101/2024.  
588 01.24.576848](https://doi.org/10.1101/2024.01.24.576848).
- 589 Jetz, W., G. H. Thomas, J. B. Joy, K. Hartmann, and A. O. Mooers (2012). “The global  
590 diversity of birds in space and time”. In: *Nature* 491.7424, pp. 444–448. DOI: [10.  
591 1038/nature11631](https://doi.org/10.1038/nature11631).
- 592 Khurana, Mark P., Neil Scheidwasser-Clow, Matthew J. Penn, Samir Bhatt, and David  
593 A. Duch ene (2023). “The Limits of the Constant-rate Birth–Death Prior for Phylo-

- 594 genetic Tree Topology Inference”. In: *Systematic Biology* 73 (1), pp. 235–246. DOI:  
595 [10.1093/sysbio/syad075](https://doi.org/10.1093/sysbio/syad075).
- 596 Lewitus, Eric, Lucie Bittner, Shruti Malviya, Chris Bowler, and H el ene Morlon (2018).  
597 “Clade-specific diversification dynamics of marine diatoms since the Jurassic”. In:  
598 *Nature Ecology & Evolution* 2.11, pp. 1715–1723. DOI: [10.1038/s41559-018-](https://doi.org/10.1038/s41559-018-0691-3)  
599 [0691-3](https://doi.org/10.1038/s41559-018-0691-3).
- 600 Maliet, Odile, Florian Hartig, and H el ene Morlon (2019). “A model with many small  
601 shifts for estimating species-specific diversification rates”. In: *Nature Ecology &*  
602 *Evolution* 3.7, pp. 1086–1092. DOI: [10.1038/s41559-019-0908-0](https://doi.org/10.1038/s41559-019-0908-0).
- 603 Maliet, Odile and H el ene Morlon (2021). “Fast and Accurate Estimation of Species-  
604 Specific Diversification Rates Using Data Augmentation”. In: *Systematic Biology*  
605 71.2, pp. 353–366. DOI: [10.1093/sysbio/syab055](https://doi.org/10.1093/sysbio/syab055).
- 606 Moen, Daniel and H el ene Morlon (2014). “Why does diversification slow down?” In:  
607 *Trends in Ecology and Evolution* 29.4, pp. 190–197. DOI: [10.1016/j.tree.2014.](https://doi.org/10.1016/j.tree.2014.01.010)  
608 [01.010](https://doi.org/10.1016/j.tree.2014.01.010).
- 609 Morlon, H el ene, J er emy Andr eoletti, Jo elle Barido-Sottani, Sophia Lambert, Beno t  
610 Perez-Lamarque, Ignacio Quintero, Viktor Senderov, and Pierre Veron (2024). “Phy-  
611 logenetic Insights into Diversification”. In: *Annual Review of Ecology, Evolution,*  
612 *and Systematics* 55, pp. 1–21. DOI: [10.1146/annurev-ecolsys-102722-](https://doi.org/10.1146/annurev-ecolsys-102722-020508)  
613 [020508](https://doi.org/10.1146/annurev-ecolsys-102722-020508).
- 614 Morlon, H el ene, Eric Lewitus, Fabien L. Condamine, Marc Manceau, Julien Clavel,  
615 and Jonathan Drury (2016). “RPANDA: an R package for macroevolutionary analy-  
616 ses on phylogenetic trees”. In: *Methods in Ecology and Evolution* 7.5, pp. 589–597.  
617 DOI: [10.1111/2041-210x.12526](https://doi.org/10.1111/2041-210x.12526).
- 618 Nee, Sean, Edward C. Holmes, Robert M. May, and Paul H. Harvey (1994). “Extinction  
619 rates can be estimated from molecular phylogenies”. In: *Philosophical Transactions*  
620 *of the Royal Society of London. Series B: Biological Sciences* 344.1307, pp. 77–82.  
621 DOI: [10.1098/rstb.1994.0054](https://doi.org/10.1098/rstb.1994.0054).
- 622 Norstr om, Melissa M., Mattia C.F. Prosperi, Rebecca R. Gray, Annika C. Karlsson,  
623 and Marco Salemi (2012). “PhyloTempo: A Set of R Scripts for Assessing and Vi-  
624 sualizing Temporal Clustering in Genealogies Inferred from Serially Sampled Viral  
625 Sequences”. In: *Evolutionary Bioinformatics* 8, pp. 261–269. DOI: [10.4137/ebo.](https://doi.org/10.4137/ebo.s9738)  
626 [s9738](https://doi.org/10.4137/ebo.s9738).
- 627 Paradis, Emmanuel and Klaus Schliep (2019). “ape 5.0: an environment for modern  
628 phylogenetics and evolutionary analyses in R”. In: *Bioinformatics* 35.3, pp. 526–  
629 528. DOI: [10.1093/bioinformatics/bty633](https://doi.org/10.1093/bioinformatics/bty633).
- 630 Perez-Lamarque, Beno t, Maarja  pik, Odile Maliet, Ana C. Afonso Silva, Marc-  
631 Andr e Selosse, Florent Martos, and H el ene Morlon (2022). “Analysing diversifica-  
632 tion dynamics using barcoding data: The case of an obligate mycorrhizal symbiont”.  
633 In: *Molecular Ecology* 31.12, pp. 3496–3512. DOI: [10.1111/mec.16478](https://doi.org/10.1111/mec.16478).
- 634 Pybus, Oliver G. and Paul H. Harvey (2000). “Testing macro-evolutionary models  
635 using incomplete molecular phylogenies”. In: *Proceedings of the Royal Society B*  
636 267.1459, pp. 2267–2272. DOI: [10.1098/rspb.2000.1278](https://doi.org/10.1098/rspb.2000.1278).
- 637 Quintero, Ignacio, Nicolas Lartillot, and H el ene Morlon (2024). “Imbalanced specia-  
638 tion pulses sustain the radiation of mammals”. In: *Science* 384.6699, pp. 1007–1012.  
639 DOI: [10.1126/science.adj2793](https://doi.org/10.1126/science.adj2793).

- 640 Rabosky, Daniel L. (2014). “Automatic Detection of Key Innovations, Rate Shifts, and  
641 Diversity-Dependence on Phylogenetic Trees”. In: *PLOS ONE* 9.2, e89543. DOI:  
642 [10.1371/journal.pone.0089543](https://doi.org/10.1371/journal.pone.0089543).
- 643 – (2016). “Reproductive isolation and the causes of speciation rate variation in nature”.  
644 In: *Biological Journal of the Linnean Society* 118.1, pp. 13–25. DOI: [10.1111/bij.  
645 12703](https://doi.org/10.1111/bij.12703).
- 646 Rabosky, Daniel L. and Daniel R. Matute (2013). “Macroevolutionary speciation rates  
647 are decoupled from the evolution of intrinsic reproductive isolation in *Drosophila*  
648 and birds”. In: *Proceedings of the National Academy of Sciences* 110.38, pp. 15354–  
649 15359. DOI: [10.1073/pnas.1305529110](https://doi.org/10.1073/pnas.1305529110).
- 650 Rolland, Jonathan et al. (2023). “Conceptual and empirical bridges between micro-  
651 and macroevolution”. In: *Nature Ecology & Evolution* 7 (8), pp. 1181–1193. DOI:  
652 [10.1038/s41559-023-02116-7](https://doi.org/10.1038/s41559-023-02116-7).
- 653 Silvestro, Daniele, Jan Schnitzler, Lee Hsiang Liow, Alexandre Antonelli, and Nicolas  
654 Salamin (2014). “Bayesian Estimation of Speciation and Extinction from Incomplete  
655 Fossil Occurrence Data”. In: *Systematic Biology* 63.3, pp. 349–367. DOI: [10.1093/  
656 sysbio/syu006](https://doi.org/10.1093/sysbio/syu006).
- 657 Singhal, Sonal, Guarino R. Colli, Maggie R. Grundler, Gabriel C. Costa, Ivan Prates,  
658 and Daniel L. Rabosky (2022). “No link between population isolation and speciation  
659 rate in squamate reptiles”. In: *Proceedings of the National Academy of Sciences*  
660 119.4, e2113388119. DOI: [10.1073/pnas.2113388119](https://doi.org/10.1073/pnas.2113388119).
- 661 Singhal, Sonal, Huateng Huang, Maggie R. Grundler, María R. Marchán-Rivadeneira,  
662 Iris Holmes, Pascal O. Title, Stephen C. Donnellan, and Daniel L. Rabosky (2018).  
663 “Does Population Structure Predict the Rate of Speciation? A Comparative Test  
664 across Australia’s Most Diverse Vertebrate Radiation”. In: *The American Naturalist*  
665 192.4, pp. 432–447. DOI: [10.1086/699515](https://doi.org/10.1086/699515).
- 666 Stadler, Tanja (2011). “Simulating Trees with a Fixed Number of Extant Species”. In:  
667 *Systematic Biology* 60.5, pp. 676–684. DOI: [10.1093/sysbio/syr029](https://doi.org/10.1093/sysbio/syr029).
- 668 – (2013). “Recovering speciation and extinction dynamics based on phylogenies”. In:  
669 *Journal of Evolutionary Biology* 26.6, pp. 1203–1219. DOI: [10.1111/jeb.12139](https://doi.org/10.1111/jeb.12139).
- 670 Virtanen, Pauli et al. (2020). “SciPy 1.0: Fundamental Algorithms for Scientific Com-  
671 puting in Python”. In: *Nature Methods* 17, pp. 261–272. DOI: [10.1038/s41592-  
672 019-0686-2](https://doi.org/10.1038/s41592-019-0686-2).

## 673 Appendices

### 674 A1 Resolution of the probability of extinction of an incipient lineage

675 In [equation 3](#), let us do the variable change  $v = t - u$  to get rid of the variable  $t$  in the  
676 integral:

$$\begin{aligned}
 677 \quad p_E^I(t) &= \frac{\mu_2}{\Lambda}(1 - e^{-\Lambda t}) + \int_0^t \lambda_3 e^{-\Lambda(t-v)} (p_E^I(v))^2 dv \\
 678 \quad &= \frac{\mu_2}{\Lambda}(1 - e^{-\Lambda t}) + \lambda_3 e^{-\Lambda t} \int_0^t e^{\Lambda v} (p_E^I(v))^2 dv \\
 679 \quad &= \frac{\mu_2}{\Lambda}(1 - e^{-\Lambda t}) + \lambda_3 e^{-\Lambda t} f(t)
 \end{aligned}$$

680 with  $f$  defined with, for all  $t \geq 0$ :

$$681 \quad f(t) := \int_0^t e^{\Lambda v} (p_E^I(v))^2 dv.$$

682 We note that

$$\begin{aligned}
 683 \quad f'(t) &= e^{\Lambda t} (p_E^I(t))^2 \\
 684 \quad &= e^{\Lambda t} \left( \frac{\mu_2}{\Lambda}(1 - e^{-\Lambda t}) + \lambda_3 e^{-\Lambda t} f(t) \right)^2.
 \end{aligned}$$

685 This is a non-linear ordinary differential equation (ODE) of first order, with the initial  
686 condition  $f(0) = 0$ . With the help of Wolfram Mathematica we have the solution:

$$687 \quad f(t) = e^{\Lambda t} \left[ \frac{1}{\lambda_3^2 (c e^{kt} + \frac{1}{k})} - \frac{\Lambda(k - \Lambda) + 2\mu_2 \lambda_3}{2\lambda_3^2 \Lambda} \right] + \frac{\mu_2}{\lambda_3 \Lambda}$$

688 with  $k = \sqrt{\Lambda^2 - 4\lambda_3 \mu_2}$  and  $c = \frac{2}{k - \Lambda} - \frac{1}{\Lambda}$  a constant to satisfy the initial condition.

689 The probability of extinction  $p_E^I(t)$  can be retrieved:

$$\begin{aligned}
 690 \quad p_E^I(t) &= \sqrt{e^{-\Lambda t} f'(t)} \\
 691 \quad &= \frac{1}{\lambda_3} \sqrt{\frac{c(\Lambda - k)e^{kt} + \Lambda/k}{(c e^{kt} + 1/k)^2} - \frac{\Lambda(k - \Lambda) + 2\mu_2 \lambda_3}{2}}.
 \end{aligned}$$

### 692 A2 Resolution of the probability of completion of an incipient lin- 693 eage

694 To get rid of the variable  $t$  in the integral of [equation 4](#), we do the change of variable  
695  $v = t - u$ . This gives us:

$$\begin{aligned}
 696 \quad 1 - p_C^I(t) &= \frac{\mu_2}{\Lambda}(1 - e^{-\Lambda t}) + e^{-\Lambda t} + \int_0^t \lambda_3 e^{-\Lambda(t-v)} (1 - p_C^I(v))^2 dv \\
 697 \quad &= \frac{\mu_2}{\Lambda}(1 - e^{-\Lambda t}) + e^{-\Lambda t} + e^{-\Lambda t} \int_0^t \lambda_3 e^{\Lambda v} (1 - p_C^I(v))^2 dv
 \end{aligned}$$



698 we now do a logarithmic change of variable in the integral,  $z = e^{\Lambda v}$ :

$$\begin{aligned}
 699 \quad &= \frac{\mu_2}{\Lambda}(1 - e^{-\Lambda t}) + e^{-\Lambda t} + e^{-\Lambda t} \int_1^{e^{\Lambda t}} \lambda_3 z \left(1 - p_C^I\left(\frac{\log z}{\Lambda}\right)\right)^2 \frac{1}{\Lambda z} dz \\
 700 \quad &= \frac{\mu_2}{\Lambda}(1 - e^{-\Lambda t}) + e^{-\Lambda t} \left(1 + \frac{\lambda_3}{\Lambda} g(e^{\Lambda t})\right)
 \end{aligned}$$

701 with, for  $x \geq 1$ :

$$702 \quad g(x) := \int_1^x \left(1 - p_C^I\left(\frac{\log z}{\Lambda}\right)\right)^2 dz.$$

703 Noting that  $g'(x) = [1 - p_C^I(\log x/\Lambda)]^2$ , we have:

$$704 \quad g'(x) = \left[ \frac{\mu_2}{\Lambda} \left(1 - \frac{1}{x}\right) + \frac{1}{x} \left(1 + \frac{\lambda_3}{\Lambda} g(x)\right) \right]^2.$$

705 This is a non-linear ODE. With the initial condition  $g(1) = 0$ , it can be solved numeri-  
706 cally and we retrieve the probability of completion of an incipient lineage with

$$707 \quad p_C^I(t) = 1 - \sqrt{g'(e^{\Lambda t})}.$$

### 708 **A3 Resolution of the probability of extinction of a good lineage**

709 From [equation 5](#) we do the same change of variable as in the previous part  $v = t - u$ :

$$710 \quad p_E^G(t) = \frac{\mu_1}{\Theta}(1 - e^{-\Theta t}) + \lambda_1 e^{-\Theta t} \int_0^t e^{\Theta v} p_E^I(v) p_E^G(v) dv$$

711 then with  $z = e^{\Theta v}$  we have:

$$\begin{aligned}
 712 \quad &= \frac{\mu_1}{\Theta}(1 - e^{-\Theta t}) + \lambda_1 e^{-\Theta t} \int_1^{e^{\Theta t}} z p_E^I\left(\frac{\log z}{\Theta}\right) p_E^G\left(\frac{\log z}{\Theta}\right) \frac{1}{\Theta z} dz \\
 713 \quad &= \frac{\mu_1}{\Theta}(1 - e^{-\Theta t}) + \frac{\lambda_1}{\Theta} e^{-\Theta t} \int_1^{e^{\Theta t}} p_E^I\left(\frac{\log z}{\Theta}\right) p_E^G\left(\frac{\log z}{\Theta}\right) dz \\
 714 \quad &= \frac{\mu_1}{\Theta}(1 - e^{-\Theta t}) + \frac{\lambda_1}{\Theta} e^{-\Theta t} h(e^{\Theta t})
 \end{aligned}$$

715 with, for  $x \geq 1$

$$716 \quad h(x) = \int_1^x p_E^I\left(\frac{\log z}{\Theta}\right) p_E^G\left(\frac{\log z}{\Theta}\right) dz.$$

717 We note that

$$\begin{aligned}
 718 \quad &h'(x) = p_E^I\left(\frac{\log x}{\Theta}\right) p_E^G\left(\frac{\log x}{\Theta}\right) \\
 719 \quad &= p_E^I\left(\frac{\log x}{\Theta}\right) \times \left[ \frac{\mu_1}{\Theta} \left(1 - \frac{1}{x}\right) + \frac{\lambda_1}{\Theta} \frac{1}{x} h(x) \right]. \quad (8)
 \end{aligned}$$

720 With the condition  $h(1) = 0$ , [equation 8](#) gives the ODE satisfied by  $h$ . If we solve this  
721 equation numerically we can retrieve  $p_E^G(t)$ :

$$722 \quad p_E^G(t) = \frac{h'(e^{\Theta t})}{p_E^I(t)}.$$

#### 723 **A4 Resolution of the probability of speciation of a good lineage**

724 From [equation 6](#), we do the same change of variable  $v = t - u$ , then  $z = e^{\Theta v}$ :

$$\begin{aligned} 725 \quad p_S^G(t) &= \lambda_1 e^{-\Theta t} \int_0^t e^{\Theta v} [p_C^I(v) + (1 - p_C^I(v))p_S^G(v)] dv \\ 726 \quad &= \lambda_1 e^{-\Theta t} \int_1^{e^{\Theta t}} z \left[ p_C^I\left(\frac{\log z}{\Theta}\right) + \left(1 - p_C^I\left(\frac{\log z}{\Theta}\right)\right) p_S^G\left(\frac{\log z}{\Theta}\right) \right] \frac{1}{\Theta z} dz \\ 727 \quad &= \frac{\lambda_1}{\Theta} e^{-\Theta t} \int_1^{e^{\Theta t}} \left[ p_C^I\left(\frac{\log z}{\Theta}\right) + \left(1 - p_C^I\left(\frac{\log z}{\Theta}\right)\right) p_S^G\left(\frac{\log z}{\Theta}\right) \right] dz \\ 728 \quad &= \frac{\lambda_1}{\Theta} e^{-\Theta t} m(e^{\Theta t}) \end{aligned}$$

729 with, for  $x \geq 0$

$$730 \quad m(x) := \int_1^x \left[ p_C^I\left(\frac{\log z}{\Theta}\right) + \left(1 - p_C^I\left(\frac{\log z}{\Theta}\right)\right) p_S^G\left(\frac{\log z}{\Theta}\right) \right] dz.$$

731 We note that

$$732 \quad m'(x) = p_C^I\left(\frac{\log x}{\Theta}\right) + \left(1 - p_C^I\left(\frac{\log x}{\Theta}\right)\right) p_S^G\left(\frac{\log x}{\Theta}\right) \quad (9)$$

$$733 \quad = p_C^I\left(\frac{\log x}{\Theta}\right) + \left(1 - p_C^I\left(\frac{\log x}{\Theta}\right)\right) \frac{\lambda_1}{\Theta} \frac{1}{x} m(x). \quad (10)$$

734 With the initial condition  $m(1) = 0$ , the [equation 10](#) gives the ODE satisfied by  $m$ . If  
735 we solve this equation numerically we can retrieve  $p_S^G(t)$  with the derivative of the  
736 solution  $m$ , from [equation 9](#):

$$737 \quad p_S^G(t) = \frac{m'(e^{\Theta t}) - p_C^I(t)}{1 - p_C^I(t)}.$$

738 We show an example of the obtained numerical solutions of  $p_E^I, p_C^I, p_E^G$  and  $p_S^G$  and  
739 empirical probabilities from simulations in supplementary figure S1.

740 **A5 Calculation of the time-constant BD rates under the PBD model**

741 **Speciation probability and expected time for speciation under the BD model**

742 Under the BD model with parameters  $\lambda$  and  $\mu$ , the probability of speciation of a given  
743 lineage is the probability that a birth event occurs before a death event, *i.e.*

744 
$$\mathbb{P}(\text{speciation}) = \frac{\lambda}{\lambda + \mu}. \quad (11)$$

745 Conditionally on speciation, the expected time  $T$  it takes for a given lineage to speciate  
746 is

747 
$$\mathbb{E}[T|\text{speciation}] = \frac{1}{\lambda + \mu} \quad (12)$$

748 since  $T$  has the same distribution as  $\min(X, Y)$  with  $X \leftrightarrow \mathcal{E}(\lambda)$  and  $Y \leftrightarrow \mathcal{E}(\mu)$  two in-  
749 dependent clock variables representing speciation and extinction events. The minimum  
750 of two exponential independent processes is distributed exponentially with a parameter  
751 equal to the sum of the rates.

752 **Speciation probability and expected time for speciation under the PBD model**

753 Under the PBD model, a good lineage speciates if it generates at least one incipient  
754 lineage and one of these incipient lineages or one of the descendants of these lineages  
755 completes speciation.

756 Considering one incipient lineage  $L$  that has still no descendent, there are two out-  
757 comes: (i) the lineage or one of its descendent at least complete speciation (we will  
758 denote this event as “complete”), or (ii) nor the lineage or any of its descendent com-  
759 plete speciation before dying (we will denote this event as “does not complete”).

760 Let us denote  $\pi := \mathbb{P}(L \text{ does not complete})$  and  $N$  the number of direct descendants  
761 of the lineage before it dies or completes speciation, and  $L$  and  $L_1, \dots, L_N$  those lineages.  
762 All the possible events that can happen to  $L$  (completion at rate  $\lambda_2$ , new incipient line-  
763 age at rate  $\lambda_3$  or extinction at rate  $\mu_2$ ) are independent point process. The first one to  
764 happen is therefore a point process with rate  $\lambda_2 + \lambda_3 + \mu_2$  and the probability that it is  
765 the formation of an incipient lineage is  $\lambda_3/(\lambda_2 + \lambda_3 + \mu_2)$ . We can thus decompose:

766 
$$\begin{aligned} \pi &= \sum_{n=0}^{+\infty} \mathbb{P}(L \text{ has } n \text{ children}) \mathbb{P}(L \text{ dies}) \prod_{i=1}^n \mathbb{P}(L_i \text{ does not complete}) \\ &= \sum_{n=0}^{+\infty} \left( \frac{\lambda_3}{\lambda_2 + \lambda_3 + \mu_2} \right)^n \frac{\mu_2}{\lambda_2 + \lambda_3 + \mu_2} \pi^n. \end{aligned}$$

767

768 Therefore

769 
$$\pi = \frac{\mu_2}{\lambda_2 + \lambda_3 + \mu_2} \times \frac{1}{1 - \frac{\pi \lambda_3}{\lambda_2 + \lambda_3 + \mu_2}} \Leftrightarrow \pi^2 - \pi \frac{\lambda_2 + \lambda_3 + \mu_2}{\lambda_3} + \frac{\mu_2}{\lambda_3} = 0.$$

770 The solution of this equation in  $[0, 1]$  is

$$771 \quad \pi = \frac{1}{2} \frac{\lambda_2 + \lambda_3 + \mu_2}{\lambda_3} \left( 1 - \sqrt{1 - 4 \frac{\lambda_3 \mu_2}{(\lambda_2 + \lambda_3 + \mu_2)^2}} \right). \quad (13)$$

772 Let us now consider a good lineage. Ignoring the proportion  $\pi$  of incipient daughter  
773 lineages that will not complete, we can consider the filtered point process with rates of  
774 successful initiation  $(1 - \pi)\lambda_1$  and extinction  $\mu_1$ . Therefore the probability of speci-  
775 ation is the probability that a successful initiation occurs before the extinction, given  
776 by:

$$777 \quad \mathbb{P}(\text{speciation}) = \frac{(1 - \pi)\lambda_1}{\mu_1 + (1 - \pi)\lambda_1}. \quad (14)$$

778 The speciation time is the branching time of the first successful incipient lineage to  
779 speciate. Therefore the speciation time is distributed as the result of the filtered point  
780 process and has the expected value:

$$781 \quad \mathbb{E}[T|\text{speciation}] = \frac{1}{(1 - \pi)\lambda_1 + \mu_1}. \quad (15)$$

## 782 **Expression of the equivalent rates of speciation and extinction**

783 The equivalent rates of BD are the rates such that  $\mathbb{P}(\text{speciation})$  and  $\mathbb{E}[T|\text{speciation}]$   
784 are equal in both models. To do so, we set  $\tilde{\lambda}$  and  $\tilde{\mu}$  such that the pairs of expressions  
785 in [equation 11/14](#) and [12/15](#) are equal. This gives us:

$$786 \quad \begin{aligned} \tilde{\lambda} &= \frac{\mathbb{P}(\text{speciation})}{\mathbb{E}[T|\text{speciation}]} \\ &= (1 - \pi)\lambda_1 \end{aligned} \quad (16)$$

788 and

$$789 \quad \begin{aligned} \tilde{\mu} &= \frac{1 - \mathbb{P}(\text{speciation})}{\mathbb{E}[T|\text{speciation}]} \\ &= \mu_1. \end{aligned}$$

## 791 **A6 Analysis of parameters limiting the equivalent birth rate**

792 We measure the influence of variation in each of the parameters of the PBD model  
793 on the equivalent birth rate  $\tilde{\lambda}$ . Parameters that influence  $\tilde{\lambda}$  the most can be considered  
794 potentially limiting, as they can drive  $\tilde{\lambda}$  down depending on their values. We calculated  
795 the partial derivatives of  $\tilde{\lambda}$ , given by the expression [equation 16](#), with respect to the  
796 PBD parameters  $\lambda_1, \lambda_2, \lambda_3$  and  $\mu_2$ .  $\mu_1$ , denoting the rate of extinction of a good lineage,  
797 has no influence on the equivalent birth rate.

$$\begin{aligned}
 798 \quad \frac{\partial \hat{\lambda}}{\partial \lambda_1} &= (1 - \pi), \quad \frac{\partial \hat{\lambda}}{\partial \lambda_2} = -\lambda_1 \frac{\partial \pi}{\partial \lambda_2}, \quad \frac{\partial \hat{\lambda}}{\partial \lambda_3} = -\lambda_1 \frac{\partial \pi}{\partial \lambda_3}, \\
 799 \quad \text{and} \quad \frac{\partial \hat{\lambda}}{\partial \mu_2} &= -\lambda_1 \frac{\partial \pi}{\partial \mu_2}.
 \end{aligned}$$

800 In what follow, we explicit the expressions (*i*, *ii* and *iii*) of the three partial derivatives  
 801 of  $\pi$  with respect to the three parameters of the incipient lineages. From [equation 13](#)  
 802 we remind  $\pi = \Lambda \left( 1 - \sqrt{1 - 4\lambda_3\mu_2/\Lambda^2} \right) / 2\lambda_3$  with  $\Lambda = \lambda_2 + \lambda_3 + \mu_2$ .

$$\begin{aligned}
 803 \quad (i) \quad \frac{\partial \pi}{\partial \lambda_2} &= \frac{1}{2\lambda_3} \left( 1 - \sqrt{1 - 4\frac{\lambda_3\mu_2}{\Lambda^2}} \right) + \frac{\Lambda}{2\lambda_3} \left( \frac{-\frac{8\lambda_3\mu_2}{\Lambda^3}}{2\sqrt{1 - 4\frac{\lambda_3\mu_2}{\Lambda^2}}} \right) \\
 804 \quad &= \frac{\pi}{\Lambda} - \frac{2\mu_2}{\Lambda\sqrt{\Lambda^2 - 4\lambda_3\mu_2}}, \\
 805 \quad (ii) \quad \frac{\partial \pi}{\partial \lambda_3} &= \frac{1}{2} \frac{\lambda_3 - \Lambda}{\lambda_3^2} \left( 1 - \sqrt{1 - 4\frac{\lambda_3\mu_2}{\Lambda^2}} \right) + \frac{\Lambda}{2\lambda_3} \times \left( -\frac{\partial u}{\partial \lambda_3} \frac{1}{2\sqrt{1 - 4\frac{\lambda_3\mu_2}{\Lambda^2}}} \right)
 \end{aligned}$$

with  $u$  defined as  $1 - 4\frac{\lambda_3\mu_2}{\Lambda^2}$ , so  $\frac{\partial u}{\partial \lambda_3} = 4\mu_2 \frac{\lambda_3 - \lambda_2 - \mu_2}{\Lambda^3}$ , hence

$$\begin{aligned}
 806 \quad \frac{\partial \pi}{\partial \lambda_3} &= -\frac{\lambda_2 + \mu_2}{2\lambda_3^2} \left( 1 - \sqrt{1 - 4\frac{\lambda_3\mu_2}{\Lambda^2}} \right) + \frac{\Lambda}{4\lambda_3} \frac{4\mu_2\Lambda}{\Lambda^3\sqrt{1 - 4\frac{\lambda_3\mu_2}{\Lambda^2}}} \\
 807 \quad &= -\frac{\lambda_2 + \mu_2}{\Lambda\lambda_3} \pi + \frac{\mu_2}{\lambda_3\Lambda^2} \frac{\lambda_2 + \mu_2 - \lambda_3}{\sqrt{1 - 4\frac{\lambda_3\mu_2}{\Lambda^2}}}, \quad \text{and} \\
 808 \quad (iii) \quad \frac{\partial \pi}{\partial \mu_2} &= \frac{1}{2\lambda_3} \left( 1 - \sqrt{1 - 4\frac{\lambda_3\mu_2}{\Lambda^2}} \right) - \frac{\Lambda}{2\lambda_3} \frac{\partial u}{\partial \mu_2} \frac{1}{2\sqrt{1 - 4\frac{\lambda_3\mu_2}{\Lambda^2}}}
 \end{aligned}$$

with  $\frac{\partial u}{\partial \mu_2} = -4\lambda_3 \frac{\lambda_2 + \lambda_3 - \mu_2}{\Lambda^3}$ , so

$$809 \quad \frac{\partial \pi}{\partial \mu_2} = \frac{\pi}{\Lambda} + \frac{\lambda_2 + \lambda_3 - \mu_2}{\Lambda^2\sqrt{1 - 4\frac{\lambda_3\mu_2}{\Lambda^2}}}.$$

810 We then use the simplified framework of the PBD model where all rates of initiation  
 811 are equal ( $b := \lambda_1 = \lambda_3$ ) and all rates of population extinction are equal ( $e := \mu_1 = \mu_2$ ).  
 812 By the chain rule:

$$813 \quad \frac{\partial \tilde{\lambda}}{\partial b} = \frac{\partial \tilde{\lambda}}{\partial \lambda_1} + \frac{\partial \tilde{\lambda}}{\partial \lambda_3} \quad \text{and} \quad \frac{\partial \tilde{\lambda}}{\partial e} = \frac{\partial \tilde{\lambda}}{\partial \mu_1} + \frac{\partial \tilde{\lambda}}{\partial \mu_2}.$$

814 We then evaluate the relative influence of a parameter as the ratio between the absolute  
815 partial derivatives. For instance the relative influence of the rate of initiation  $b$  is:

$$816 \quad \text{relative influence}(b) = \frac{\left| \frac{\partial \hat{\lambda}}{\partial b} \right|}{\left| \frac{\partial \hat{\lambda}}{\partial b} \right| + \left| \frac{\partial \hat{\lambda}}{\partial \lambda_2} \right| + \left| \frac{\partial \hat{\lambda}}{\partial e} \right|}.$$

817 We provided a detailed plot of the values of this relative influence of the 3 simplified  
818 parameters in supplementary figure S5. The summary of these relative influences is  
819 provided on [figure 4](#). A similar analysis with the detailed model (with  $\lambda_1 \neq \lambda_3$  and  
820  $\mu_1 \neq \mu_2$  a priori) was also done (supplementary figure S6).